High-Performance Autofocusing for Light-Weight SAR Platforms

Ievgen M. Gorovyi, Oleksandr O. Bezvesilniy and Dmytro M. Vavriv
Department of Microwave Electronics, Institute of Radio Astronomy of NAS of Ukraine
4 Chervonopraporna Str., Kharkov 61002, Ukraine
email:gorovoy@rian.kharkov.ua, tel.: +380668205318

Abstract— **autofocusing is one of the key steps in the high-resolution SAR imaging. In the paper several important improvements to the recently developed local-quadratic map-drift autofocus are proposed. Important SAR image preprocessing steps applied before the local Doppler rate errors estimation are described. The weighting scheme for the evaluation of residual cross-track acceleration components is developed. It is illustrated that accounting of the local image contrast leads to better estimation precision. Also it is shown that the usage of measured real antenna orientation angles results in more reliable estimation of the local Doppler rate errors. Performance of the trajectory reconstruction technique is tested with experimental data obtained with X-band airborne SAR system.**

Keywords—synthetic aperture radar; autofocus; Doppler rate errors; residual trajectory deviations

I. INTRODUCTION

The quality of synthetic aperture radar (SAR) images essentially depends on the trajectory measurements performed by the navigation system [1]-[4]. With the rapid development of high-resolution imaging systems autofocusing becomes one of the most important steps of the SAR data processing. Since in order to obtain well-focused SAR images of the scene, platform deviations should be known with sub-wavelength precision, requirements to the applied autofocus techniques are very strict as well [5]-[6].

Recently a novel approach for the arbitrary phase error estimation was developed [7]. The method is called local-quadratic map-drift autofocus (LQMDA). Its basic idea is related with the usage of the Doppler rate error estimates on short-time intervals with subsequent reconstruction of the residual arbitrary phase error function. It was shown that such local estimation can be performed via the well-known map-drift algorithm (MDA) [5], [7]-[8] modified for the case of the SAR processing on a short-time interval. The proposed approach can be applied for both stripmap and spotlight modes and does not require the existence of bright targets on the scene. This gives several benefits in comparison to the existing nonparametric techniques [3], [9]-[10]. On the other hand, the developed method performs the parametric estimation only within the short-time intervals and proper combining of the local estimates provides a possibility to retrieve the arbitrary phase error function.

In the paper we consider several important practical improvements to the LQMDA approach. In particular, for better precision of local Doppler error estimation, several SAR image preprocessing steps are proposed. The weighting scheme for the evaluation of the residual cross-track acceleration from the sequence of the local Doppler rate errors is introduced. It is shown that in this case the contributions from image areas with different contrast can be properly balanced. For the additional improvement of local Doppler rate errors estimation the measured real antenna orientation angles are incorporated. As a result, the developed technique can provide a high-precise reconstruction of the SAR platform residual deviations. Together with improvements proposed in the paper, the LQMDA becomes an efficient tool for the estimation of an arbitrary range-dependent phase errors from the SAR data and image refocusing.

In Section II, improvements for the SAR processing on a short-time interval and local Doppler rate estimation are considered. The ideas of how the high-precise trajectory reconstruction can be achieved are proposed in Section III. In particular, the weighting scheme for the processing of range-blocks for the local trajectory restoration is described. The main stages of the improved autofocus algorithm and examples of obtained real SAR images are illustrated in Section IV.

II. LOCAL MAP-DRIFT ALGORITHM AND PRECISE DOPPLER RATE ERROR ESTIMATION

In general, an unknown residual phase error has an arbitrary nature. According to the developed autofocus technique, fragments of the phase error function can be described via local approximations as

$$\varphi_E(R,t_n+\tau) \approx \varphi_E(R,t_n) + \varphi'_E(R,t_n)\tau + \varphi''_E(R,t_n)\tau^2/2 \quad (1)$$

Here R corresponds to a particular range gate, t_n is the center of the considered short-time interval of duration T_S, τ is the time within the short interval.

It can be shown that the value of the local-quadratic phase error $\varphi''_E(R,t_n)$ (proportional to the Doppler rate error F^E_{DR}) can be estimated via the application of the local MDA to the SAR images pair built on the considered short-time interval

[7]. In order to improve the efficiency of the local estimation, we propose to use the Dechirp algorithm [3], [11] instead of recently described range-Doppler algorithm specifically modified for such SAR processing [7], [12]. In this case the pair of SAR images can be formed as follows

$$I_1(f) = \frac{2}{T_S} \int_{-T_S/2}^{0} w_S(\tau + T_S/4) s(\tau) h^*(\tau) \exp[-2\pi i f \tau] d\tau \,, \quad (2a)$$

$$I_2(f) = \frac{2}{T_S} \int_{0}^{T_S/2} w_S(\tau - T_S/4) s(\tau) h^*(\tau) \exp[-2\pi i f \tau] d\tau \,. \quad (2b)$$

Here $w_S(\tau)$ is a weighting window, $h(\tau)$ is a time-domain reference function. Hence, in such case the images can be obtained using only single short Fourier transform. At the next step, the accurately measured linear shift $\Delta f_{\max}$ between the images can be used to determine the value of the Doppler rate error

$$F_{DR}^{E} = 2\Delta f_{\max} / T_S \,. \quad (3)$$

A common approach for the shift estimation is the cross-correlation of the SAR images pair. An important thing is to ensure a precise estimation of the cross-correlation peak position. In order to fulfill these requirements we propose to apply several image preprocessing steps. At first, the images are recalculated into a logarithmic scale and the dynamic range is narrowed (Fig. 1).

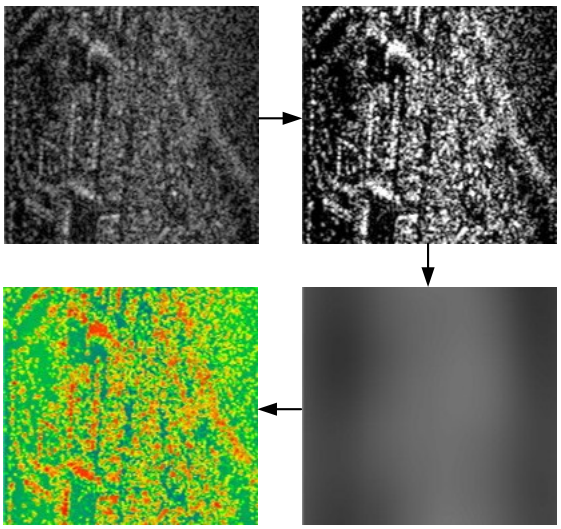

Figure 1. SAR images preprocessing steps.

This allows to balance the contributions from bright and dark image features. At the next step the local centering is performed. Such operation can be written as

$$I_{\mathrm{LC}}(X_k, R_n) = I_{\mathrm{LDR}}(X_k, R_n) - I_{\mathrm{blurred}}(X_k, R_n) \,, \quad (4)$$

where I_{LDR} is the SAR image with narrowed dynamic range, I_{blurred} is blurred version of the image.

The application of above described preprocessing steps solves the problem of a strong influence of large-scale objects and bright artificial targets, which significantly affects on the cross-correlation results. In this case it is possible to obtain sharp peaks of resulting cross-correlation functions which provides a high-precision estimate for the cross-correlation peak position. As a result, the local Doppler rate errors are extracted much more precisely.

III. Improvements of Local Trajectory Deviations Reconstruction

A. Weighting Scheme for Estimation of Acceleration Components

Another challenge in SAR imaging from light-weight platforms is range-dependence of the residual phase error function. This is especially important in the case of low-altitude and wide-range-swath SAR systems.

In order to handle the range-dependence of the residual phase error, the sequence of the estimated Doppler rate errors $F_{DR}^{E}(R, t_n)$ within several range-blocks can be used for the evaluation of the unknown residual acceleration errors. It was found that the main contribution to the Doppler rate error is related with the cross-track acceleration components $a_Y(t_n), a_Z(t_n)$ [7]. As a result, the following simple expression for the Doppler rate error at slant range R can be used

$$F_{DR}^{E}(R, t_n) \approx \frac{2}{\lambda} \frac{y_R a_Y(t_n) - H a_Z(t_n)}{R} \,, \quad (5)$$

where

$$y_R = -H \tan\alpha \sin\beta + \cos\beta \sqrt{R^2 - H^2 - (H \tan\alpha)^2} \,, \quad (6)$$

H is a flight altitude, α, β are the antenna pitch and yaw angles, respectively.

Based on Doppler rate error (5) calculated for the sequence of the range blocks, the mean square estimator (MSE) can be constructed as

$$MSE(a_Y(t_n), a_Z(t_n)) = \\ = \sum_{m=1}^{M_R} w_m(t_n) \left[\frac{2}{\lambda} \frac{y_{R_m} a_Y(t_n) - H a_Z(t_n)}{R_m} - F_{DR}^{E}(R_m, t_n) \right]^2 \,, \quad (7)$$

where R_m is the central range gate of each range block, and $F_{DR}^{E}(R_m, t_n)$ are the estimated Doppler rate errors.

In contrast to the original estimation scheme [13], additional weighting coefficients $w_m(t_n)$ are introduced.

Their values correspond to the cross-correlation functions maxima for each of range block m. The usage of such weighting allows to provide more reliable and precise local reconstruction of the residual cross-track acceleration. This can be achieved because the cross-correlation peak position can be estimated more accurately within the range-blocks with higher image contrast.

An example of calculated weighting coefficients $w_m(t_n)$ and defocused SAR image is illustrated in Fig. 2. One can observe the correspondence between the image contrast level and the value of cross-correlation maxima.

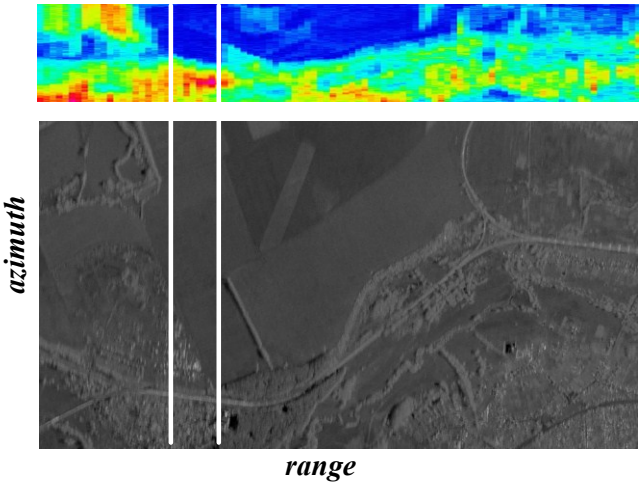

Figure 2. Cross-correlation maxima and defocused SAR image.

Proposed weighting scheme allows to balance the contributions from image areas with different contrast and improve the overall efficiency of the developed autofocusing technique.

The cross-correlation function for each range block m is calculated as an average of the cross-correlation functions for all range gates within this block:

$$R_{CC}^{m}(m,\Delta X)=\frac{1}{N_{RB}}\sum_{n=0}^{N_{RB}-1}R_{CC}(\,R_{mN_{RB}+n},\Delta X)\,. \qquad (8)$$

Here N_{RB} is the number of range gates in the range block, $R_{CC}(\,R_n,\Delta X)$ is a cross-correlation function for the particular range gate. As a result, introduced averaging leads to the speckle noise variance reduction in $\sqrt{N_{RB}}$ times.

B. Incorporation of Measured Real Antenna Orientation Angles

The efficiency of the proposed trajectory reconstruction algorithm can be additionally improved using the measured real antenna orientation angles α,β. Since the light-weight SAR platforms demonstrate both trajectory deviations and antenna orientation instabilities, the usage of the fixed orientation angles for the consequent local estimations on the short-time intervals can lead to the additional bias of the local Doppler rate error F_{DR}^{E}.

Assuming that the average antenna orientation angles are fixed to zero ($\overline{\alpha}=\overline{\beta}=0$), one can derive a simple expression for the bias of the Doppler rate error estimate

$$\Delta F_{DR}^{E}(t_n R,\alpha_n,\beta_n)=\frac{2a_Y(t_n)}{\lambda R}*$$
$$*\left[H\tan\alpha_n\sin\beta_n+\sqrt{R^2-H^2}-\cos\beta_n\sqrt{R^2-\frac{H^2}{\cos^2\alpha_n}}\right]. \qquad (9)$$

Here α_n,β_n are the values of the antenna pitch and yaw corresponding to the center of a particular short-time interval. One can see that the above mentioned bias is a function of the cross-track acceleration component a_Y, the slant range R and flight altitude H as well.

Described Doppler rate error bias (9) has an important influence and should be accounted at the local phase error estimation step.

IV. Experimental Results

This section contains the description of the main stages of the improved trajectory reconstruction approach. As usual, we assume that the conventional SAR processing steps including the range-compression, the motion compensation based on the navigation system measurements and range-cell migration correction (RCMC) are applied to the SAR raw data buffer. Fig. 3 illustrates the block-scheme of the proposed trajectory reconstruction method.

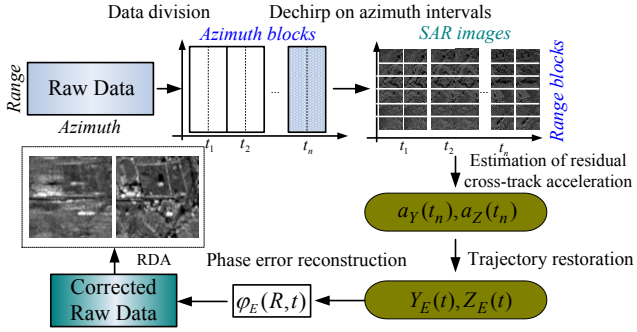

Figure 3. Block-scheme of developed trajectory reconstruction approach.

At first, SAR image pairs are built on a sequence of short-time intervals. This is performed using the Dechirp algorithm. For each short-time interval the developed weighting scheme is applied for the evaluation of the residual cross-track acceleration components. The residual trajectory deviations are reconstructed via double integration of the evaluated residual acceleration time-series. At the next step the range-dependent phase error function is calculated and properly compensated in the SAR data. Finally, the corrected SAR data

can be processed by a conventional SAR focusing algorithm (range-Doppler algorithm [3] is a good option).

Fig. 4 illustrates an example of real SAR images obtained with the airborne RIAN-SAR-X system [14] developed and produced at the Institute of Radio Astronomy of the National Academy of Sciences of Ukraine.

The left image is a result of the SAR processing based on the trajectory measurements. Significant defocusing is observed. The right image is an example of the application of

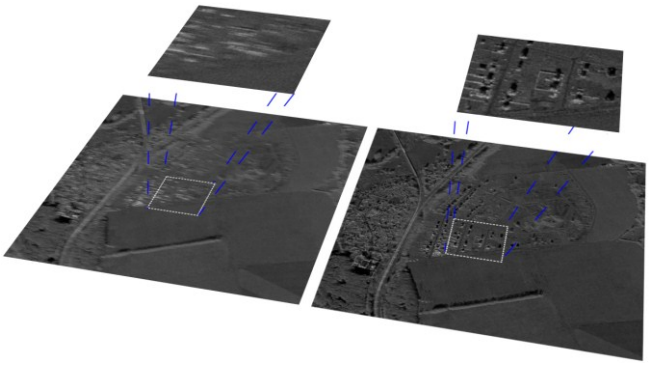

Figure 4. Illustration of SAR image refocusing (25 looks, 1-m resolution, left – before autofocusing, right – after autofocusing).

the proposed trajectory reconstruction procedure. The comparison of small image patches clearly indicates that the detailing level is significantly improved. Also the geometric shapes and fine details are successfully refocused after the application of the developed reconstruction technique.

V. CONCLUSION

In the paper, important practical improvements for the recently developed autofocus algorithm are introduced. In particular, accounting of the local image contrast in the proposed weighting scheme provides more reliable cross-track acceleration evaluation. Incorporation of the measured real antenna orientation angles provides more precise estimates for the local Doppler rate errors on short-time intervals. Proposed improvements for the full trajectory reconstruction allow to efficiently handle an arbitrary range-dependent phase errors caused by an unstable movement of the SAR platform. The application of the developed technique is especially important for the high-resolution imaging from light-weight platforms and allows to considerably improve the efficiency of the existing SAR systems.

REFERENCES

[1] C. Oliver and S. Quegan, Understanding Synthetic Aperture Radar Images. Norwood, MA: Artech House, 1999.

[2] G. Franceschetti and R. Lanari, Synthetic Aperture Radar Processing. CRC Press, 1999.

[3] W. G. Carrara, R. S. Goodman, and R. M. Majewski, Spotlight Synthetic Aperture Radar: Signal Processing Algorithms. Boston; London: Artech House, 1995.

[4] I. G. Cumming and F. H. Wong, Digital Processing of Synthetic Aperture Radar Data: Algorithms and Implementation". Norwood, MA: Artech House, 2005.

[5] P. Samczynski and K. Kulpa, "Coherent MapDrift technique", IEEE Trans. on Geoscience and Remote Sensing, vol. 48, no. 3, pp. 1505–1517, March 2010.

[6] O.O. Bezvesilniy, I.M. Gorovyi and D.M. Vavriv, "Effects of local phase errors in multi-look SAR images", Progress In Electromagnetics Research B, Vol. 53, pp.1-24, 2013.

[7] O.O. Bezvesilniy, I.M. Gorovyi and D.M. Vavriv, "Estimation of phase errors in SAR data by local-quadratic map-drift autofocus", Proc. 13th Int. Radar Symp. IRS-2012, Warsaw, Poland, pp. 376-381, 2012.

[8] H. M. J. Cantalloube and C. E. Nahum, "Multiscale local map-drift-driven multilateration SAR autofocus using fast polar format algorithm image synthesis", IEEE Trans. on Geoscience and Remote Sensing, vol. 49, no. 10, pp. 3730–3736, Oct 2010.

[9] D.E. Wahl, P.H. Eichel, D.C. Ghiglia, and C.V. Jakowatz, Jr., "Phase gradient autofocus – A robust tool for the high-resolution phase correction", IEEE Trans. Aerosp. Electron. Syst., vol. 30, no. 3, pp. 827-835, 1994.

[10] V.C. Koo, T.S. Lim, and H.T. Chuah, "A comparison of autofocus algorithms for SAR imagery", Progress In Electromagnetics Research Symposium, pp. 16-19, 2005.

[11] J. Wang, D. Cai and Y. Wen., "Comparison of matched filter and dechirp processing used in Linear Frequency Modulation", IEEE International Conference on Computing, Control and Industrial Engineering , Vol. 2, pp. 70-73, 2011.

[12] I.M. Gorovyi, O.O. Bezvesilniy and D.M. Vavriv, "Modifications of Range-Doppler Algorithm for Compensation of SAR Platform Motion Instabilities", International Journal of Electronics and Telecommunications, Vol. 60, no. 3, pp.225-231, 2014.

[13] O.O. Bezvesilniy, I.M. Gorovyi, D.M. Vavriv, 2013, "Efficient estimation of residual trajectory deviations from SAR data", In Proceedings of the 10th European Radar Conference (EURAD 2013), Nuremberg, Germany, pp. 188-191.

[14] D. M. Vavriv at al., "X-band SAR system for light-weight Aircrafts", Proc. 15th Int. Radar Symp. IRS-2014, Gdansk, Poland, pp. 501–505, 2014.